CFD-Simulation of the Combustion Process in the Mascotte Facility under Supercritical Conditions

M. Poschner, I. Zimmermann, M. Pfitzner

Universität der Bundeswehr, München
Fakultät für Luft- und Raumfahrttechnik
Institut für Thermodynamik
Werner-Heisenberg-Weg 39, 85577 Neubiberg

1 Introduction

Modern high performance rocket combustion engines are operated with cryogenic propellants at high pressures in order to improve the specific momentum. Typically, cryogenic hydrogen as fuel and liquid oxygen as oxidiser are injected separately into the combustion chamber, and burn as a diffusion flame. Oxygen is here in an overcritical condition because the pressure is above the critical one, although the temperature is subcritical.
Complex flow phenomena appear especially near by the injector, where besides the turbulent mixing process and chemical reactions also real gas effects have to be considered. Above the critical pressure liquid and gaseous phases are no longer separated. Near the critical point small changes of state have great effects on transport properties and variables of state, leading to huge gradients in the density and other thermodynamic variables during the mixing of two overcritical fluids. Turbulent structures in the mixing layer can be seen in subcritical as well as supercritical injections, but ligaments and droplets develop only in subcritical injection.

These extreme conditions can not be predicted accurately by commercial CFD-Codes yet, because at such low temperatures the material properties of oxygen can no longer be described as an ideal gas and real gas effects appearing at the mixing process of hydrogen and oxygen are thermodynamically not treated correctly by the codes available today.

The material properties of hydrogen and oxygen are reviewed more precisely below, focusing on the implementation into commercial CFD-Codes. The commercial CFD-Code ANSYS-CFX is validated at the test case RCM-2 measured on the Mascotte test bench (V03), built up by the ONERA and fired first in 1998.

2 Real gas properties of H2 and O2

The phase of a pure substance can be identified from the phase diagram. Figure 1 shows a schematic phase diagram. The melting curve represents the phase change from solid to liquid (or supercritical), the sublimation curve from solid to gaseous and the vapour pressure curve from liquid to gaseous. The intersection point of those three lines is called triple point. Here all three phases coexist. The critical point on the upper end of the vapour pressure curve is defined by the critical temperature T_c, pressure p_c and density ρ_c. Above the critical point ($T > T_c \vee p > p_c$) liquid and gaseous phase are no longer separated. The critical point of hydrogen is T_c = 33.25 K, p_c = 12.97 bar and ρ_c = 31.014 kg/m^3. The critical point of oxygen is T_c = 154.581 K, p_c = 50.43 bar and ρ_c = 436.129 kg/m^3.

Figures 2 and 3 compare the data provided by the ‚National Institute of Standards and Technology (NIST)' [1] with those resulting from the equation of state for ideal gases and the Redlich-Kwong equation of state [2], which is implemented in numerous commercial CFD-Codes:

Correspondence to : maria-magdalena.poschner@unibw.de

$$p = \frac{RT}{v-b} - \frac{a}{v(v-b)\sqrt{T}}$$

here p is the pressure, T is the temperature, v is the specific volume, R is the specific gas constant and a and b are constants depending on the regarded material.

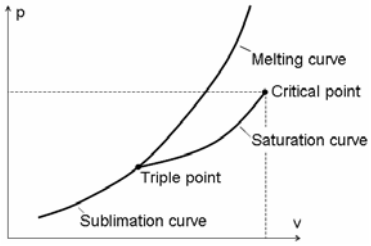

Figure 1: Phase diagram

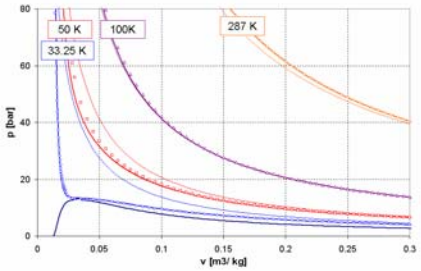

Figure 2: pv-diagram of hydrogen

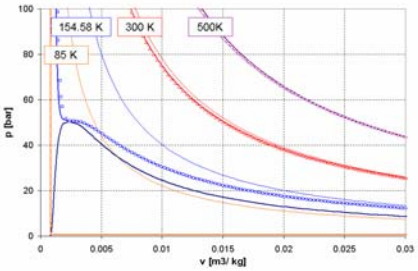

Figure 3: pv-diagram of oxygen

In the pv-diagram of hydrogen and oxygen the thick lines represent the data provided by NIST, the thin lines result from the equation of state for ideal gases and the points apply to the Redlich-Kwong equation of state. The orange lines represent the values depending on the regarded test case. In the diagram for oxygen the differences for the 500K isotherm are negligible. Also the differences appearing at 300K are only very small. For the critical isotherm however, there are large differences between the Redlich-Kwong equation, the NIST data and the equation for ideal gases. The gas behaviour can no longer be regarded as ideal. Even the Redlich-Kwong equation of state can only describe the gas behaviour qualitatively correctly, the results especially for $v < v_c$ are not reproduced correctly. The same applies for the ideal equation of state and the NIST data for the isotherm at 85 K, which is the injection temperature of the oxygen for the regarded test case, but the Redlich-Kwong equation here provides very well fitting results. For hydrogen the Redlich-Kwong equation provides very well fitting results for the critical isotherm, but the equation of state for ideal gases is also not able to describe the gas behaviour. The isotherm at 100 K shows almost no differences for all three sets of data. But for 287 K, the injection temperature of hydrogen there are small differences between the ideal gas equation and the NIST data.

For the validation of the real gas model implemented in ANSYS CFX the Mascotte single injector Test Case RCM-2 A60' [3-4] was chosen. The boundary conditions are listed in table 1:

Conditions	H2	O2
Pressure	6 MPa	6 Mpa
Mass flow rate	70 g/s	100 g/s
Temperature	287 K	85 K
Density	5.51 kg/m^3	1177.8 kg/m^3
Velocity	236 m/s	4.35 m/s

Table 1: boundary conditions for RCM-2 A60

The injector consists of an oxygen injector element with a diameter of 3.6 mm at the inlet, diverging to a diameter of 5 mm right before the orifice. Hydrogen is injected coaxially, with an inner diameter of 5.6 mm and an outer diameter of 10 mm. The length of the injector is 50 mm in order to receive a fully developed turbulent flow profile on the injector exit. The combustion chamber has a cuboid shape of 50 mm × 50 mm × 478 mm. In our simulation it is modelled by a cylindrically shaped chamber with a radius of 28.21 mm to conserve the chamber volume.

Simulations are carried out on a 20° sector of the whole chamber. The grid used is a tetrahedral one, adapted to the expected flame shape. The injector walls were covered with prism layers for a good resolution of the near wall flow.

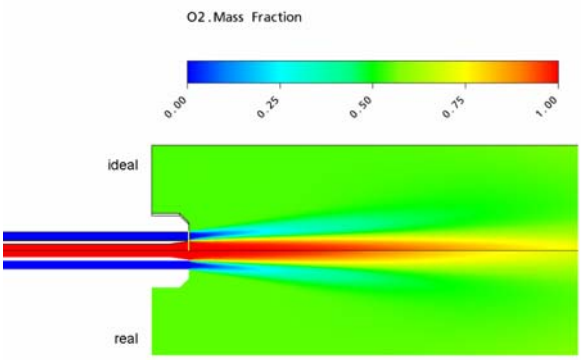

Figure 4: Comparison of oxygen mass fraction

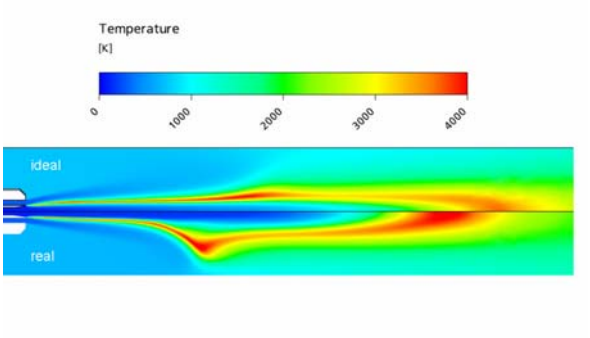

Figure 5: Comparison of flame shape

As figure 3 indicates, the density of the oxygen at those extreme conditions is predicted absolutely wrongly by the equation of state for ideal gases and therefore the injection velocity is highly over-predicted. The density resulting for oxygen regarded as ideal gas at 85 K and 60 bar is 267.7 kg/m^3 compared to the correct value of 1177.8 kg/m^3. The Redlich-Kwong equation of state (1201.77 kg/m^3) fits that value quite well. This leads to a predicted injection velocity of 21.648 m/s using the ideal equation of state which is much too high. The expected value of 4.35 m/s is slightly over-predicted by the Redlich-Kwong equation of state (4.83 m/s).

Hydrogen is regarded as ideal gas for all simulations performed. This leads to a slightly under-predicted density of 5.09 kg/m^3 and to an over-prediction in the injection velocity of 248.8 m/s. The highly under-predicted density of oxygen using the ideal equation of state has also influences on the resulting flame shape. One of the most important similarity parameters for the atomization performance and by that on the flame shape is the momentum flux ratio of the injected gas and liquid. This is miss-predicted by a factor 4, leading to a dilatation of the flame, compared to that resulting form the Redlich-Kwong equation of state.

For all further studies the gas behaviour of oxygen was modelled using the Redlich-Kwong equation of state, hydrogen was assumed to be an ideal gas.

3 Comparison of Combustion Models

The combustion model used for the simulation is of great importance for the temperature distribution resulting for the flame. The Eddy Dissipation Model used in the simulation produces much too high temperatures up to 4200 K, in reality the maximum burning temperature of oxygen and hydrogen is about 3600 K. That high temperatures result because only the reaction of hydrogen and oxygen to water is considered. Taking into account, additionally the species O, H, OH, H_2O_2, HO_2 , which are produced in reality during the combustion process of oxygen and hydrogen, the temperature drop to a maximum value of 3200 K which is much more realistic. This was predicted by the flamelet model implemented in CFX called CFX RIF.

Unfortunately there are no experimental temperature data available for this concrete case.

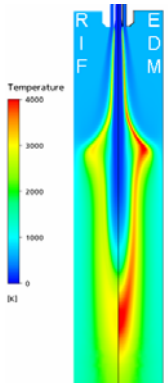

Figure 6: Temperature distribution (RIF/EDM)

4 Comparison of LOx-Distribution

One aspect for the verification of the obtained CFD results is the comparison of the LOx-Distribution right downstream of the injector.

Two shadograph pictures [5] of the LOx core right behind of the injector are compared with the oxygen mass fraction resulting from the CFD.

The LOx core is very dark in the shadowgraph pictures compared to the coaxial injected hydrogen because of its high density, which is two orders of magnitude higher than that of hydrogen. On the left side of figure 7 the mass fraction of oxygen resulting form the CFD calculation is shown. The agreement of the jet shape is very good.

The red line in figure 8 represents an isoline for an oxygen mass fraction of 1% from the CFD simulation. The CFD results fit the dark LOx core also very well for a wider area of consideration.

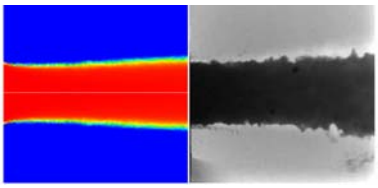

Figure 7: 17 mm × 17 mm shadowgraphy picture right behind the orifice

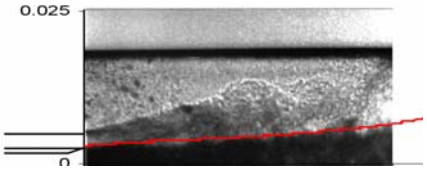

Figure 8: 50 mm × 25 mm shadowgraphy picture right behind the orifice

5 Comparison of OH-emission

Another aspect for the validation of the CFD results is the shape of the resulting flame. This can be visualized using chemiluminescence measurements where the emission of the hydroxyl radical, OH, is measured to locate regions of intense combustion. Emission images provide the instantaneous signal integrated over the line of sight. These images have to be averaged and Abel-transformed to determine the mean volumetric light intensity distribution. Qualitative results are not available here. In figure 9 the OH distribution on an intersection through the rotation axis resulting from the CFD is compared with an Abel-transformed image [6] for the test case considered. The qualitative agreement is rather good, but the flame in the CFD-simulation is slightly too long and the flame is more diverging than in the experiment. This might be caused by the simplification of the chamber where the wall is about 3.2 mm more distant to the rotation axis and the window cooling and heat loss missing still in the CFD simulation.

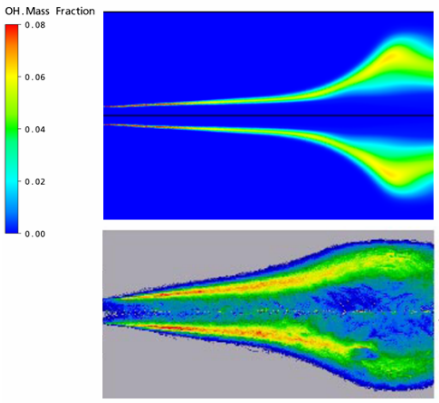

Figure 9: Comparison of OH-concentration

References

[1] E.W. Lemmon, M.O. McLinden, D.G. Friend (2005). Thermophysical Properties of Fluid Systems. NIST Chemistry WebBook, NIST Standard Reference Database Number 69, National Institute of Standards and Technology, Gaithersburg MD, 20899 (http://webbook.nist.gov)

[2] O. Redlich, J.N.S. Kwong (1949). On the Thermodynamics of Solutions. V – An Equation of State. Fugacities of Gaseous Solutions Chemical Reviewers, 44: 233-244

[3] A. Nicole, L. Vingert, M. Habiballah (2006). Test Case RCM-2, Mascotte single injector – 60 bar. 3rd International Workshop on Rocket Combustion Modelling

[4] G. Cheng, R. Farmer (2002). CFD spray combustion model for liquid rocket engine injector analyses. American Institute of Aeronautics and Astronautics, Inc. (AIAA)

[5] M. Habiballah, M. Orain, F. Grisch, L. Vingert, P. Gicquel (2006). Experimental Studies of High-pressure cryogenic Flames on the Mascotte facility. Combustion Science and Technology, 178: 101-128

[6] L. Vingert, M. Habiballah, P. Vuillermoz, S. Zurbach (2000). Mascotte, a test facility for cryogenic combustion research at high pressure. American Institute of Aeronautics and Astronautics, Inc. (AIAA)